Supplementary information for

Site-specific time-resolved FRET reveals local variations in the unfolding mechanism in an apparently two-state protein unfolding transition

Sandhya Bhatia[1], G. Krishnamoorthy[2] and Jayant B. Udgaonkar[1]*

[1]National Centre for Biological Sciences

Tata Institute of Fundamental Research

Bengaluru 560065, India.

[2]Department of Biotechnology

Anna University

Chennai 600025, India.

*Corresponding author: Professor Jayant B. Udgaonkar

National Centre for Biological Sciences

Tata Institute of Fundamental Research

Bengaluru 560065, India.

Phone: 91-80-23666150

Fax: 91-80-23636662

Email: jayant@ncbs.res.in

Running Title: Revealing site-specific deviations from two state unfolding by equilibrium multisite tr-FRET studies

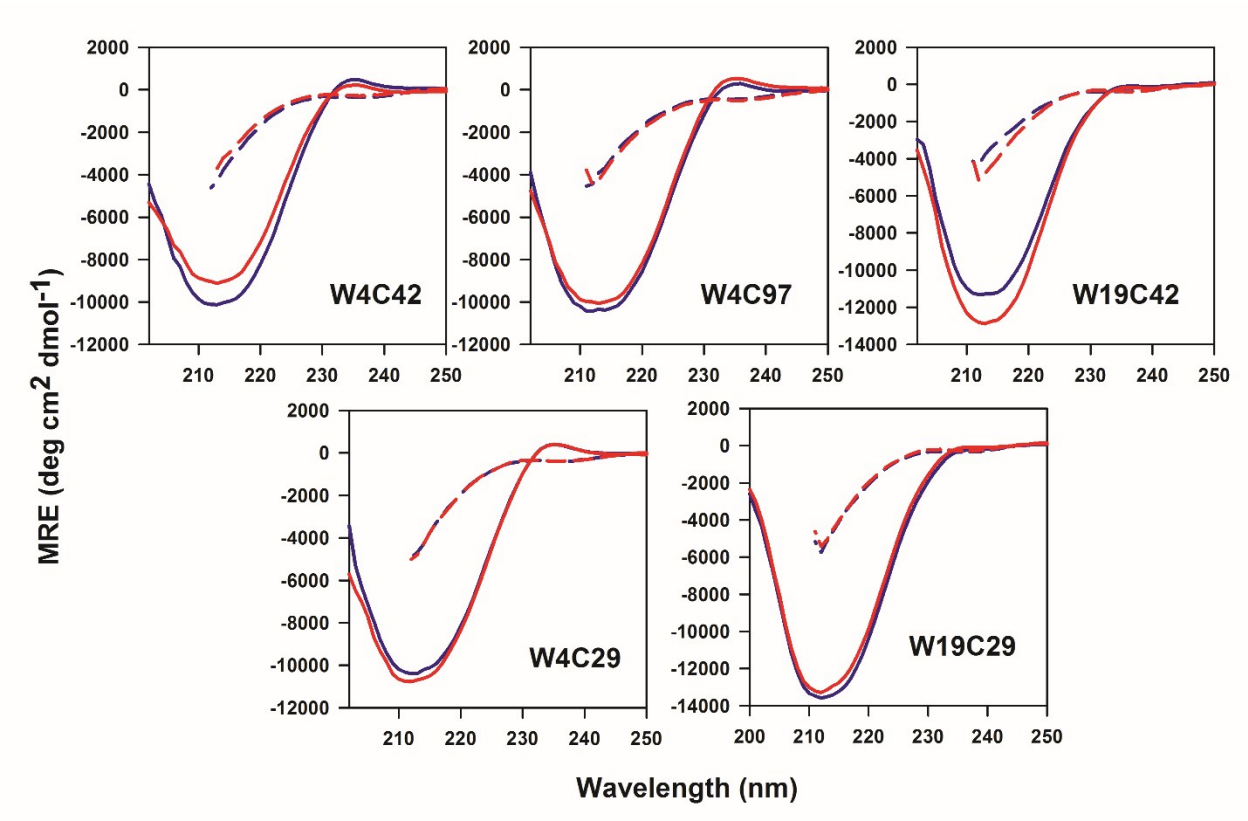

Figure S1. Far-UV CD spectra of the different mutant variants of MNEI. Spectra of the native (solid lines) and unfolded (dashed lines) states are shown for the TNB-labeled (red lines) and unlabeled (blue lines) proteins.

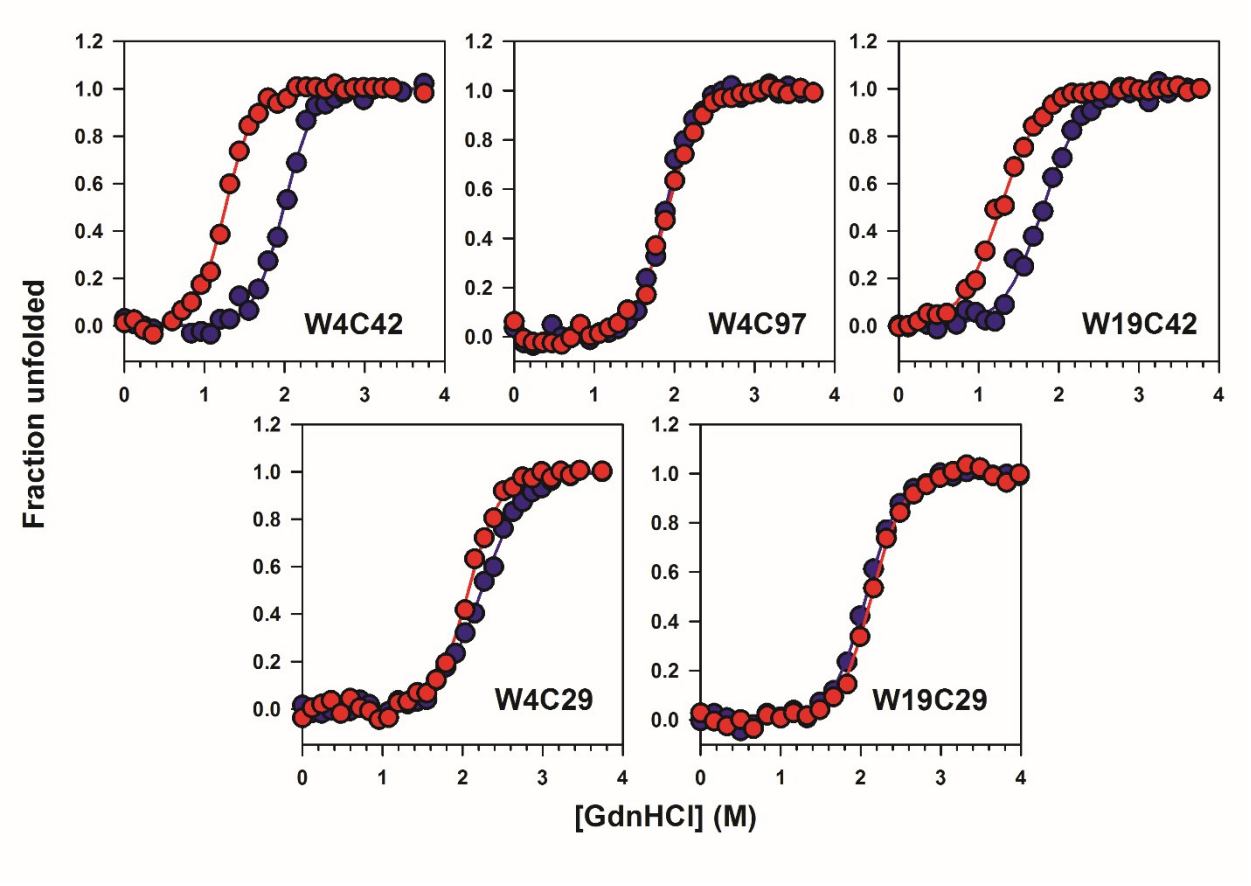

Figure S2. Equilibrium unfolding curves of the different mutant variants of MNEI measured by monitoring the far-UV CD signal at 222 nm. The blue and red circles correspond to the unlabeled and TNB-labeled protein signals, respectively. The solid line passing through each dataset is a non-linear, least-squares fit to a two-state unfolding model [1].

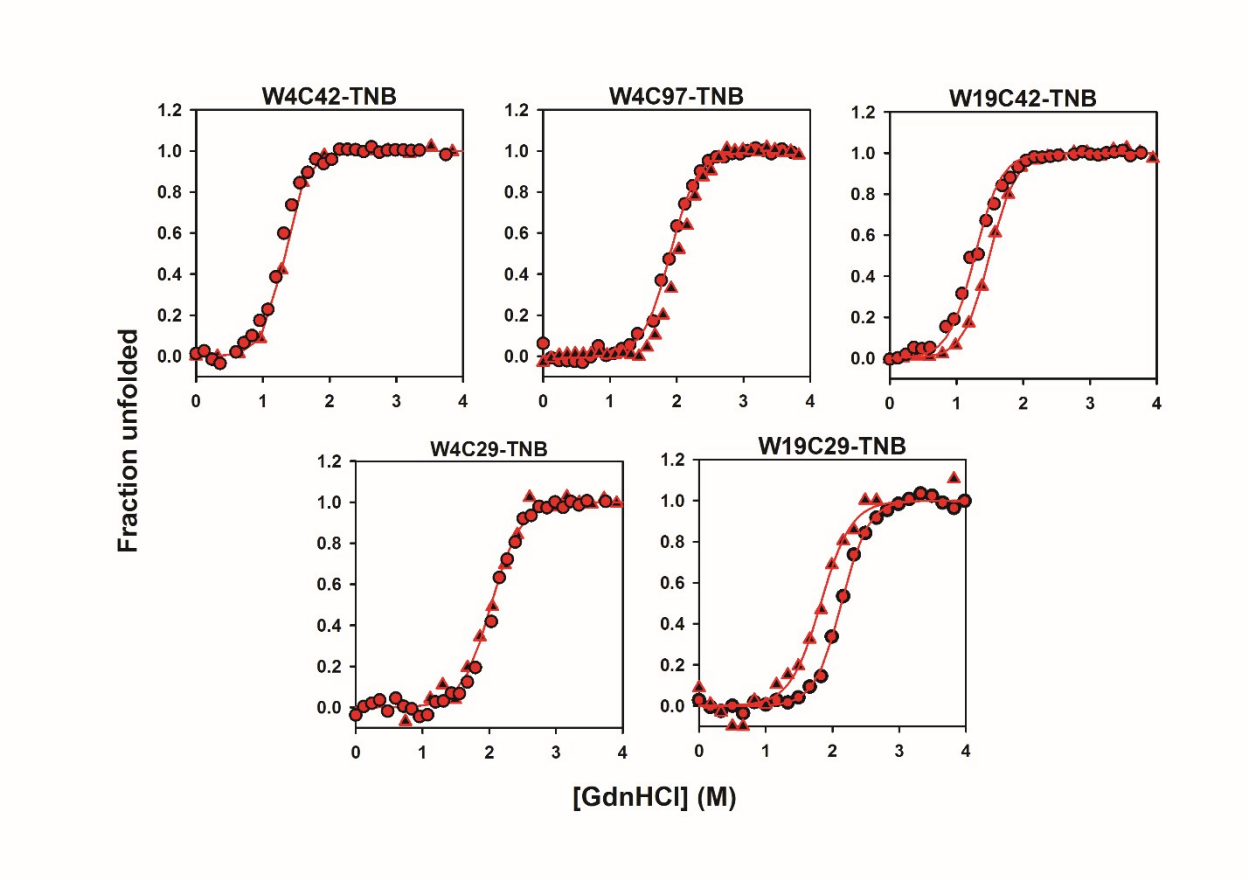

Figure S3. Equilibrium unfolding curves of the different TNB-labeled mutant variants of MNEI monitored using fluorescence at 360 nm (upright triangles) and far-UV CD at 222 nm (circles). The solid line passing through each dataset is a non-linear, least-squares fit to a two-state unfolding model [1]

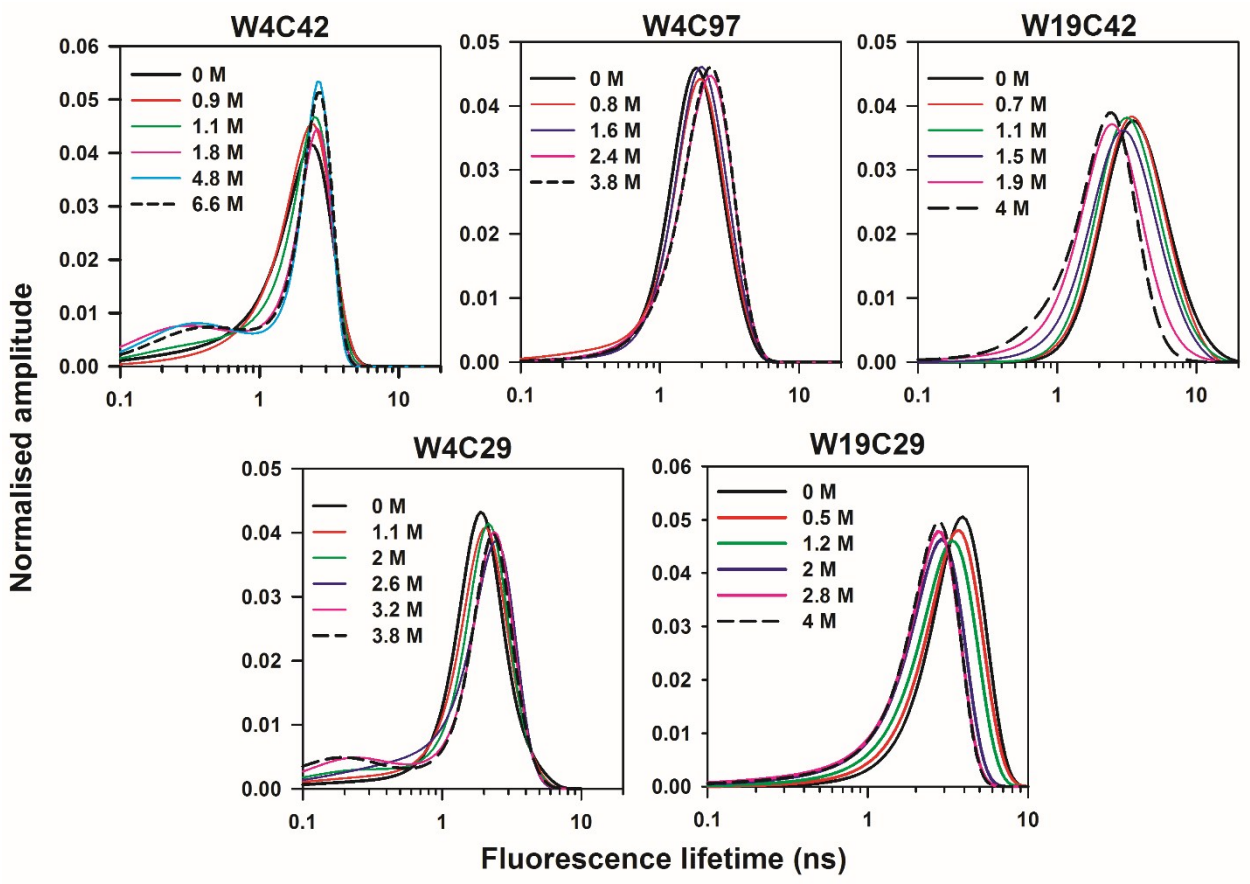

Figure S4. MEM-derived fluorescence lifetime distributions of the unlabeled mutant variants of MNEI at different GdnHCl concentrations. Different colors correspond to various concentrations of GdnHCl, as described separately in each panel. The x-axis has been plotted on a log scale. The amplitude has been normalized to the sum of amplitudes for each distribution.

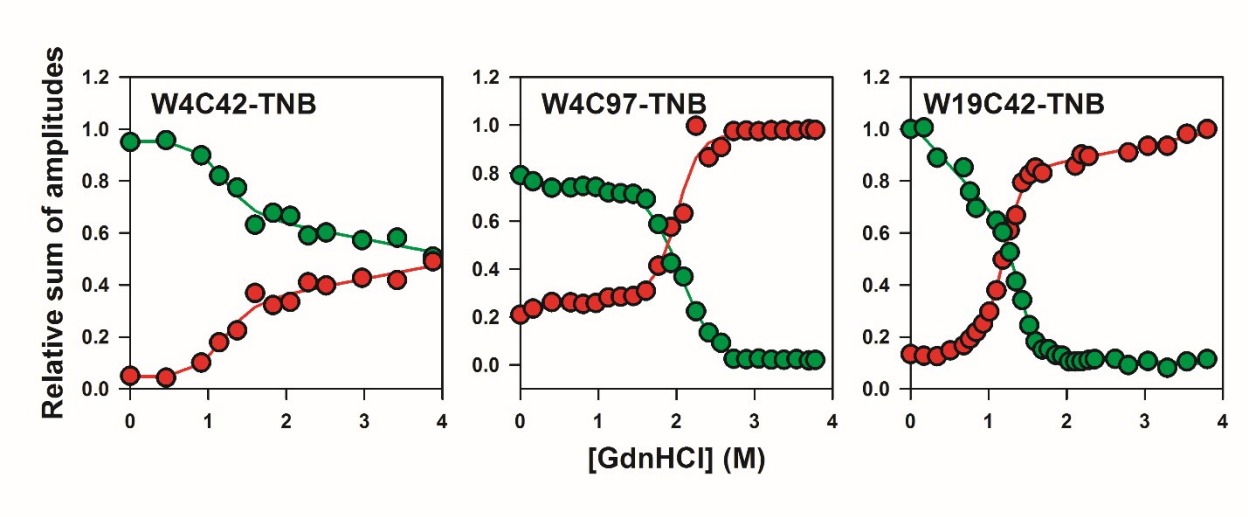

Figure S5. Cooperative changes during equilibrium unfolding monitored by the relative sum of amplitudes under the N-like and U-like distributions for three TNB-labeled proteins. The red and green circles represent the relative sum of amplitudes for the U-like and N-like populations, respectively. The relative sum of amplitudes for each population is the sum of amplitudes of the distribution for that population divided by the sum of amplitudes of the distributions for both the N-like and U-like populations. The solid line passing through each dataset is a non-linear, least-squares fit to a two-state unfolding model [1].

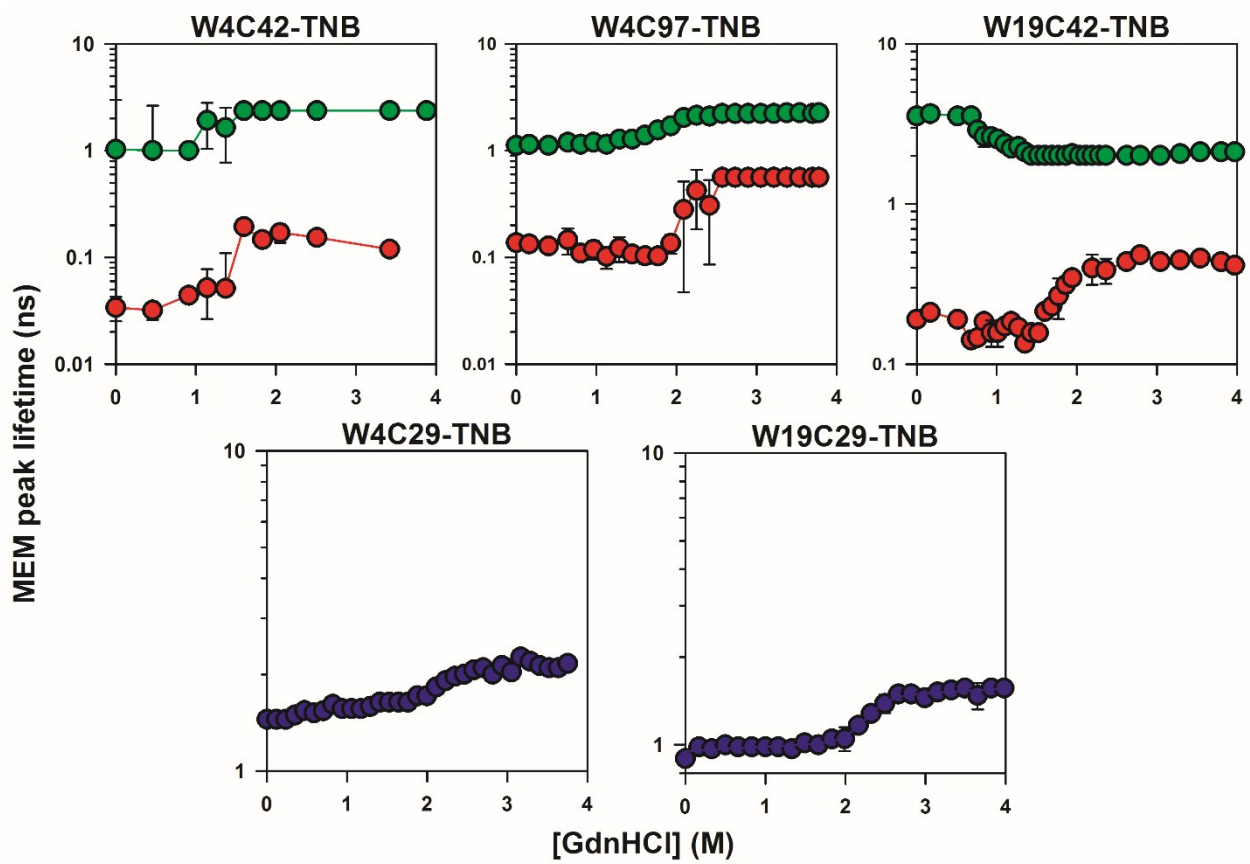

Figure S6. Quantification of the movement in the MEM peak position for the TNB-labeled proteins. Red and green circles represent the peak lifetimes of the N-like (short lifetime) and U-like (long lifetime) species, respectively. The blue symbols in the panels for W4C29-TNB and W19C29-TNB correspond to the peak position of the observed unimodal fluorescence lifetime distributions. The solid lines are drawn to guide the eye. The error bars represent the standard deviation in the measurements of the same sample from three different acquisitions. The y-axis has been plotted on a log scale.

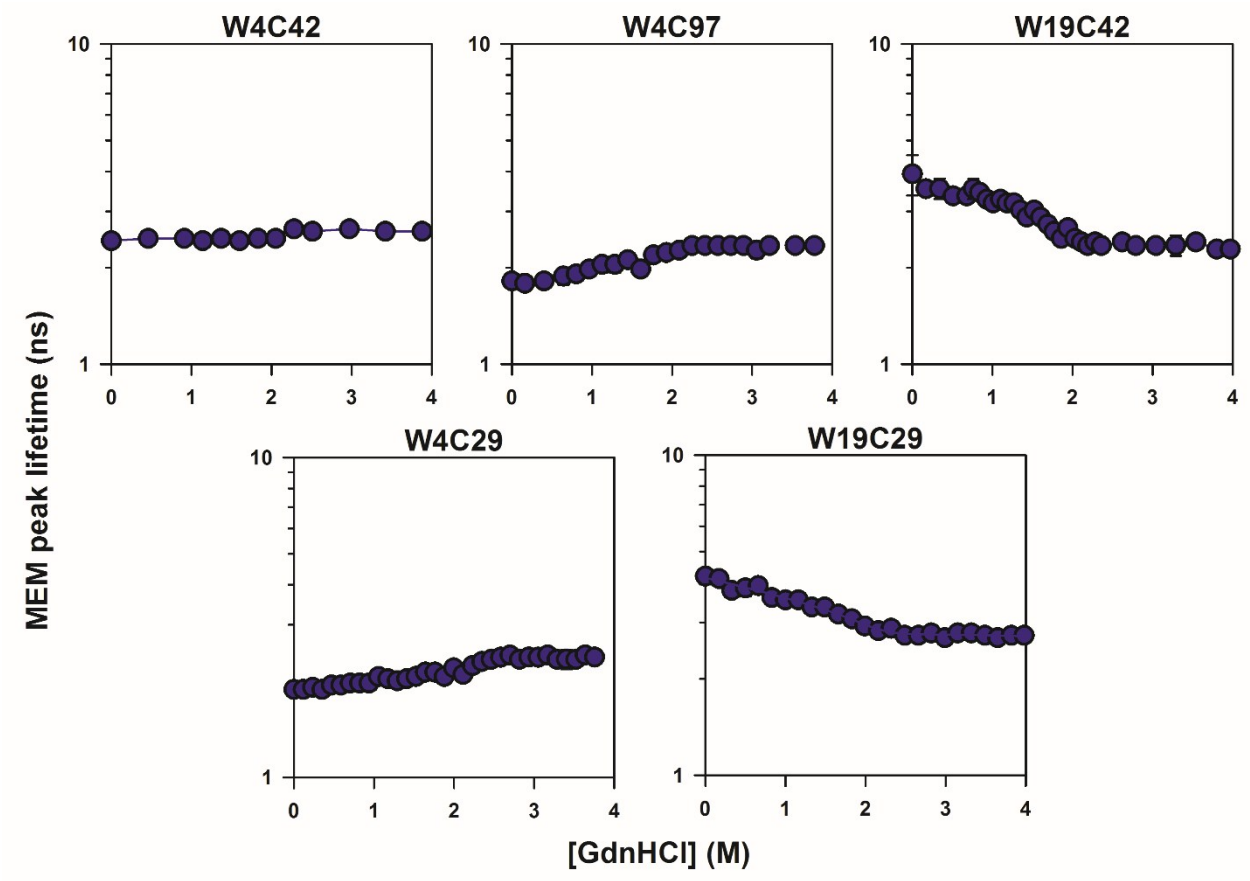

Figure S7. Quantification of the movement in the MEM peak position for all the unlabeled proteins. The blue circles represent the peak lifetimes of the observed unimodal or bimodal (in the case of W12C29) distributions. The solid lines are drawn to guide the eye. The error bars represent the standard deviations in the measurements of the same sample from three different acquisitions. The y-axis has been plotted on a log scale.

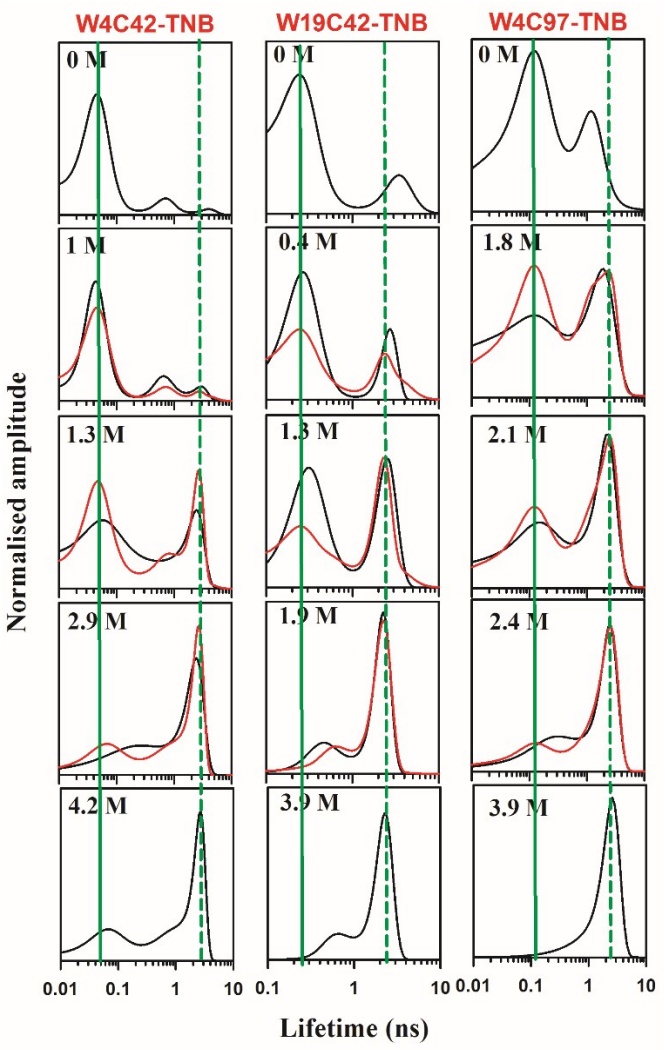

Figure S8. Non-linear, least-squares fits to a two-state N↔U model for FRET pairs spanning different regions of the β-sheet. The MEM-derived fluorescence lifetime distributions obtained at different GdnHCl concentrations (indicated at the top left of each panel) were fit to the linear sum of the native state N(τ) and unfolded state U(τ) fluorescence lifetime distributions (Eq. (6)). The black distributions correspond to the experimentally determined distributions, and the red distributions are fits to the two-state model. The top-most and bottom-most panels in each column show the fluorescence lifetime distributions used as the native N(τ) and unfolded U(τ) protein basis spectra, respectively. The vertical green lines indicate the peak positions of the N-state and U-state lifetime distributions. The x-axis has been plotted on a log scale, and the y-axis units are arbitrary. Note that the figure shows data similar to that shown in Figure 8, but from an independent experiment on different samples. The MEM distributions in Figures 8 and S8 are seen to differ in their widths for the same denaturant concentration. This is because, in general, the width of a MEM distribution is not as reproducible and robust a parameter as the peak position (see Figures S6 and S7). Nevertheless, as stated on page 28, the general trend of change in the MEM distribution, from the N to the U state, is similar in Figures 8 and S8.

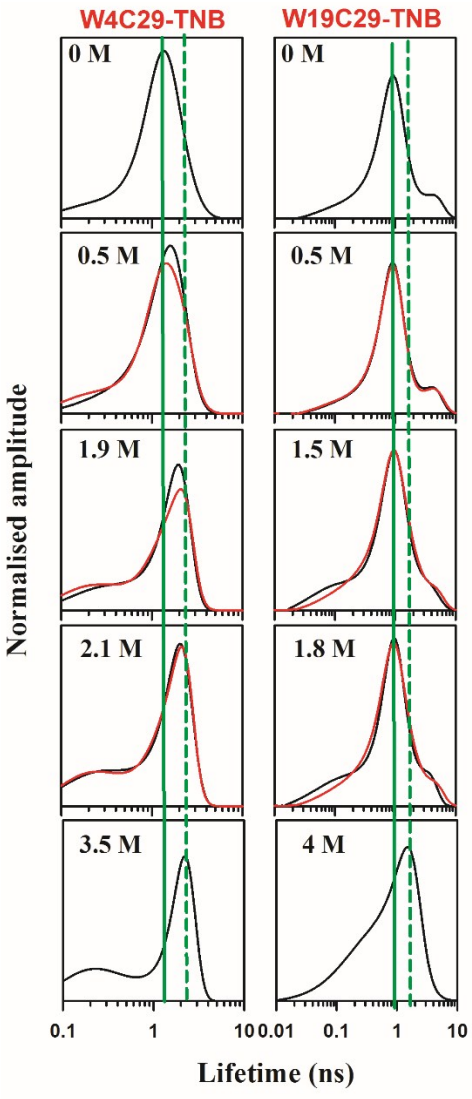

Figure S9. Non-linear, least-squares fits to a two-state N↔U model for FRET pairs spanning different regions of the α-helix. The MEM-derived fluorescence lifetime distributions obtained at different GdnHCl concentrations (indicated at the top left of each panel) were fit to the linear sum of the native state N(τ) and unfolded state U(τ) fluorescence lifetime distributions (Eq. (6)). The black distributions correspond to the experimentally determined distributions, and the red distributions are fits to the two-state model. The top-most and bottom-most panels in each column show the fluorescence lifetime distributions used as the native N(τ) and unfolded U(τ) protein basis spectra, respectively. The vertical green lines indicate the peak positions of the N-state and U-state lifetime distributions. The x-axis has been plotted on a log scale, and the y-axis units are arbitrary. Note that the figure shows data similar to that shown in Figure 9, but from an independent experiment on different samples. The MEM distributions in Figures 9 and S9 are seen to differ in their widths for the same denaturant concentration. This is because, in general, the width of a MEM distribution is not as reproducible and robust a parameter as the peak position (see Figures S6 and S7). Nevertheless, as stated on page 28, the general trend of change in the MEM distribution, from the N to the U state, is similar in Figures 9 and S9.

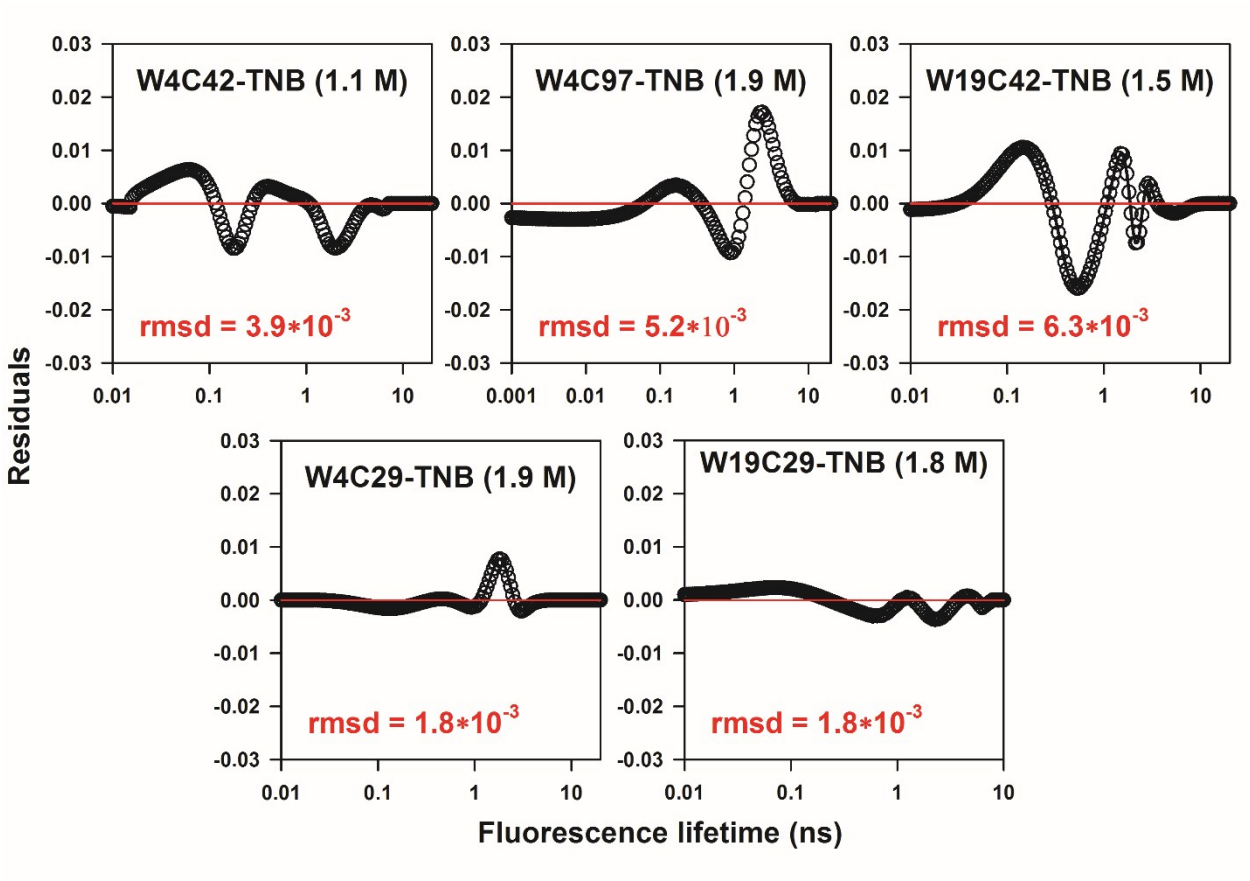

Figure S10. Quality of the fits for MEM-derived fluorescence lifetime distributions to a two-state N↔U model (Eq. (6), Figures 8 and 9). The residuals obtained for GdnHCl concentrations close to the mid-point of the unfolding transition are shown. Values in red correspond to the root mean square deviation (rmsd), which was obtained as the square root of the mean of the squares of residuals across all the lifetime values (x-axis).

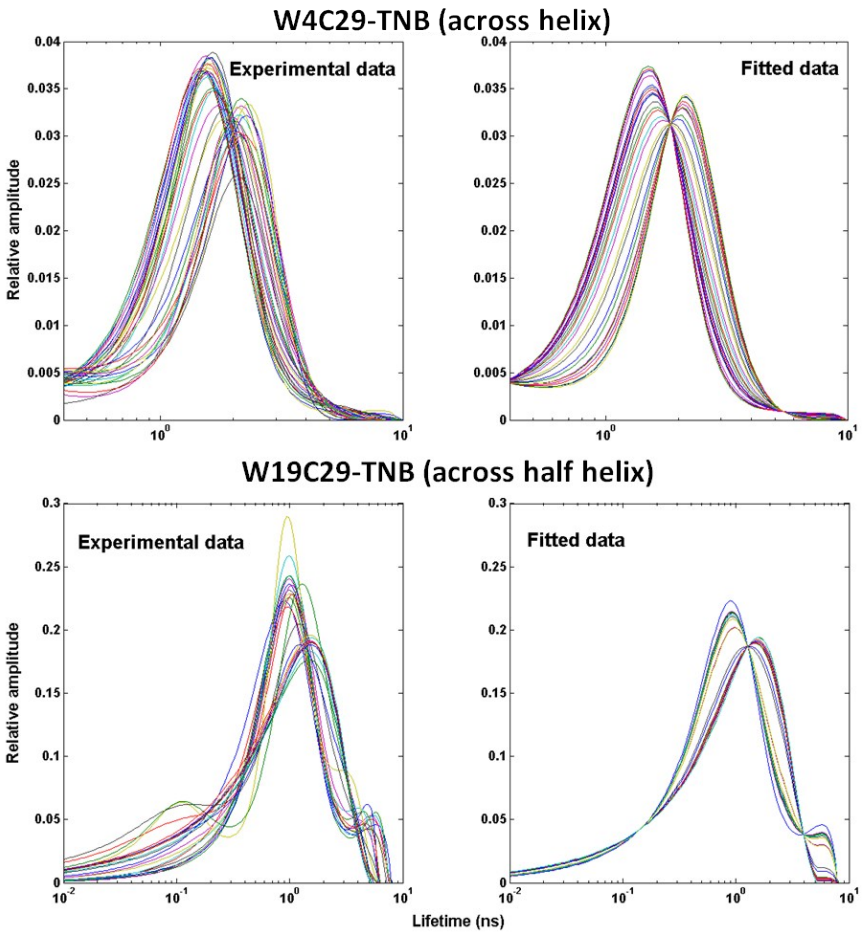

Figure S11. Fits of experimental data to a two-state N↔U model for W4C29-TNB and W19C29-TNB. The experimental data were fit to the weighted sum of the N and U state lifetime distributions (Figure 9). Different colours in all the panels correspond to varying concentrations of GdnHCl; 0 M (towards shorter lifetime) to 4 M (towards longer lifetime).

Table S1. Quantum Yields of fluorescence of the native and unfolded states.

Protein	Q_N	Q_U	$Q_U - Q_N$
W4C42	0.111	0.106	0.005
W4C42-TNB	0.005	0.067	0.062
W4C97	0.106	0.101	-0.005
W4C97-TNB	0.019	0.088	0.069
W19C42	0.208	0.122	-0.114
W19C42-TNB	0.019	0.09	0.071
W4C29	0.103	0.101	-0.002
W4C29-TNB	0.066	0.072	0.006
W19C29	0.187	0.127	0.05
W19C29-TNB	0.06	0.061	-0.001

Q_N ans Q_U values were determined using the areas under the fluorescence emission spectra.

NATA was used as the reference.

Table S2. Thermodynamic parameters obtained from fluorescence-monitored equilibrium unfolding measurements for different mutant variants of MNEI at pH 8 and 25°C.

Protein	Free energy of unfolding (ΔG_U), kcal mol^{-1}	Mid point of unfolding (C_m), M
W4C42	7.3 ± 0.6	2.16 ± 0.18
W4C42-TNB	4.4 ± 0.1	1.31 ± 0.02
W4C97	6.7 ± 0.4	1.96 ± 0.13
W4C97-TNB	6.9 ± 0.1	2.03 ± 0.01
W19C42	6.3 ± 0.1	1.86 ± 0.01
W19C42-TNB	4.9 ± 0.2	1.46 ± 0.06
W4C29	6.9 ± 0.1	2.04 ± 0.04
W4C29-TNB	7.3 ± 0.1	2.16 ± 0.03
W19C29	7.1 ± 0.1	2.10 ± 0.03
W19C29-TNB	5.8 ± 0.6	1.72 ± 0.16

Table S3. Energy transfer parameters of the native and unfolded states.

Protein	FRET efficiency	Quantum yield	Overlap integral, J*10^(-13)	Förster distance, R_0 (Å)
W4C42_N	0.94	0.1110	7.4	23.1
W4C42_U	0.10	0.1060	9.3	23.1
W19C42_N	0.83	0.2080	6.6	25.2
W19C42_U	0.16	0.1220	8.8	23.4
W4C97_N	0.75	0.1060	6.1	22.2
W4C97_U	0.11	0.1010	6.9	21.8
W4C29_N	0.28	0.1030	7.0	22.6
W4C29_U	0.15	0.1010	8.1	22.4
W19C29_N	0.61	0.1870	7.0	25.0
W19C29_U	0.45	0.1270	8.2	23.3

Table S4. Distances between the donor and acceptor residues for different FRET pairs in the native and unfolded states.

Protein	Average Förster distance, R_0 (Å)	Measured Native state distance (Å)	Calculated Native state distance (Å)	Measured Unfolded state distance (Å)	No. of residues between donor and acceptor
W4C42	23.1	14.5	13.0	33.6	38
W4C97	22.0	18.3	19.6	31.2	93
W19C42	24.3	18.6	16.1	32.1	23
W4C29	22.5	26.3	27.7	30.2	25
W19C29	24.1	22.4	18.2	25.0	10

Calculated distances correspond to the distances between the center of the donor ring and Cβ atoms of the cysteine (attached to acceptor) in the N state, obtained from the structure of MNEI using Pymol (PDB ID: 1IV7). It should be noted that the FRET-measured distance would be that separating the tryptophan from the TNB moiety attached to the cysteine. The differences in the values of the expected (from the crystal structure) and measured (from FRET) distances, for the different proteins, especially for W19C29, are likely because the TNB adduct is oriented differently (on the average) with respect to the tryptophan in the different labeled protein variants.

References

1 V. R. Agashe and J. B. Udgaonkar, Thermodynamics of Denaturation of Barstar: Evidence for Cold Denaturation and Evaluation of the Interaction with Guanidine Hydrochloride+, *Biochemistry*, 1995, **34**, 3286–3299.